A SIMULATION OF THE CLIMATIC CONDITIONS ASSOCIATED WITH THE COLLAPSE OF THE MAYA CIVILIZATION

B. G. HUNT and T. I. ELLIOTT

CSIRO Atmospheric Research, PMB1, Aspendale, Victoria 3195, Australia
E-mail: barrie.hunt@csiro.au

Abstract. It has been speculated that the collapse of the Maya civilization in the Yucatan region of Mexico around 900 AD was caused by drought. A 10,000-year simulation with the CSIRO Mark 2 coupled global climatic model has been used to investigate such a possibility. The model replicates sporadic, severe drought over the Yucatan consistent with the above speculation. It was found that these droughts were specifically constrained to the Central American area, with no obvious linkages to other regions. An investigation of the mechanisms associated with rainfall fluctuations over the Yucatan indicates that these were not caused by sea surface temperature variations. Fluctuations in the intensity of the topographically constrained meridional wind systems located on both the western and eastern coasts of the Americas were found to be the dominant influence. The sensitivity of the Yucatan to drought episodes arises from its location at the convergence zone of these wind systems. It is concluded that the severe drought episodes in this region are a consequence of stochastic fluctuations of these wind systems and that external influences are not necessary.

1. Introduction

One of the most fascinating areas of history is that concerned with the rise and fall of empires and civilizations. In many cases climate may have been a factor in the downfall of a civilization, either by direct impact, or as a consequence of invasions by people forced out of their homelands by climatic changes. A broad discussion of the role of climatic changes in such situations has been given by deMonocal (2001). This paper is concerned with the causes associated with the demise of the Maya civilization which developed on the Yucatan Peninsula of Mexico and in adjacent regions. The lifespan of this civilization was from approximately 50 BC to about 900 AD (Dahlin, 1983).

The Mayans developed an elaborate and complex society, perhaps best epitomized in the popular imagination by their magnificent temples which were constructed in the form of pyramids. Numerous pyramids survive to the present day. The Mayans had a system for writing, a complicated calendrical arrangement and employed widespread irrigation for their farming. They built substantial cities, and at its peak the population ranged into the millions (Coe, 1999).

What then caused the spectacular collapse of Maya civilization around 900 AD? Numerous possibilities have been raised at different times. These include war, as the Mayans were apparently a very warlike people. Disease, in all its possible ramifications; impoverishment of the cultivated lands due to the removal of essential

Climatic Change (2005) 69: 393–407

nutrients by over-cropping (the Mayans employed slash-and-burn agriculture); soil loss from runoff; contamination of aquifers by salt water intrusion from rising sea-levels; and over-population may also have been a contributory factor.

However, there is an emerging view (Dahlin, 1983; Hodell et al., 1995; Haug et al., 2003) that the most likely cause of the collapse was severe drought. This does not preclude any of the above causes, or other possible causes, from being contributory factors.

According to Dahlin (1983), drought may have been responsible for earlier collapses of Maya civilization. He notes the abandonment of a major Maya city in 250 AD. In addition to the short term droughts there also appear to have been longer term climatic changes. For example, Hodell et al. (1995) identify the period 5100–1000 years BC as having relatively wet conditions. This period was followed by much greater climatic variability and drier conditions.

The first definitive evidence that drought could have been associated with the Maya collapse was obtained by Hodell et al. (1995) from a lake sediment core. They state that the period 800–1000 AD was the driest in the previous 8000 years. Haug et al. (2003), using sediments from the Cariaco Basin off Venezuela as a proxy for Yucatan rainfall, have produced specific dates for major, multi-year droughts in the Yucatan. The periods involved are (all approximately) 200, 760, 810, 860 and 910 AD. The first period is associated with the pre-classical collapse and the remaining periods with the classical collapse. The relationship between the last four drought periods and the final collapse of the Maya civilizations still seems to be obscure. Haug et al. (2003) quote speculations that there was regional variability, with the collapse occurring first in the south and concluding in the north a century later.

Given that the Mayans survived the drought of 250 AD (Dahlin, 1983), a major question remains concerning why they did not recover again after the widely spaced droughts in the latter period? Haug et al. (2003) suggest it may have been related to the control of water reservoirs by Maya rulers, with the prolonged drought subsequently undermining their authority.

The combination of over population, drought and drought-related disease might represent a more plausible possibility. Drought-related disease has been hypothesized as the cause of the death of possibly 80% of the Indian population of Mexico around 1550 AD (Acuna-Soto et al., 2000). The megadrought associated with this calamity has also been replicated with the current 10,000-year simulation (Hunt and Elliott, 2002). The hemorrhagic fever that caused these deaths was specific to the Indian population, but no longer exists according to Acuna-Soto et al. (2000). Certainly, it seems unlikely that a succession of multi-year droughts, spaced fifty years apart, would have been sufficient in their own right to have caused the total collapse of the Maya civilization around 900 AD.

If disease was associated with these major droughts then this could account for the complete and permanent abandonment of Maya cities. Any survivors would be dispersed into the countryside and would probably not wish to return to the cities because of the fear of disease. Presumably with a high enough death toll

the Maya governmental system also disintegrated. A problem would still remain in accounting for the initial collapse in the south with the final termination not occurring until 150 years later in the north.

The central issue here is whether the drought scenario itself is plausible. This hypothesis can be explored using a coupled global climatic model to see whether the proposed drought scenarios can be replicated, which would then permit an investigation to be made into the causes of such droughts.

Since the CSIRO Mark 2 coupled model has been used to generate 10,000 years of simulated climate a dataset existed for such a study. The model was specifically set up so that only internally generated, naturally occurring climatic variations, attributable to non-linear mechanisms and physical processes within the model, could be produced. Thus all 'external' forcing agents such as solar variability, volcanic eruptions or greenhouse gas changes were excluded.

This limitation of the model represents a very interesting test as regards the generation of past climatic fluctuations. The natural tendency for many scientists is to search for some external forcing mechanism when trying to explain such fluctuations. For example, Hodell et al. (2001) have suggested that solar forcing may have been, at least partially, responsible for some observed droughts in the Yucatan. The formulation of the present simulation permits the role of internal climatic forcing to be uniquely identified and then compared with observed fluctuations. Where natural forcing is found wanting it is then appropriate to search for an external forcing mechanism. Of course, there may be situations, such as the Little Ice Age, where both internal and external forcing play a role (Hunt, 1998). However, the view advocated here is that when trying to understand climatic fluctuations over the last few thousand years then naturally occurring climatic variability should be given first priority, and only if this found to be inadequate should resort be made to alternative forcing agents.

In addition to the present study, the role of naturally occurring climatic variability has been used to explain a number of past, observed climatic fluctuations using a range of CSIRO global climatic models. These include studies of the Little Ice Age (Hunt, 1998), Sahelian rainfall trends (Hunt, 2000), persistent climatic anomalies (Hunt, 2001) and Mexican megadrought (Hunt and Elliott, 2002). Considerable potential exists for investigating numerous other climatic features using the output from this 10,000-year simulation.

2. Model Details

The CSIRO Mark 2 coupled global climatic model consists of atmospheric, oceanic, biospheric and sea-ice components. The horizontal resolution of the model is based on the R21 spectral formulation which implies grid boxes spaced at 5.625° longitudinally and 3.25° latitudinally. This gives a total of 3584 grid boxes per vertical level distributed over the global surface. The atmospheric and oceanic components

of the model have nine and twenty one vertical levels, respectively. These two components are coupled via radiative and heat fluxes and dynamical processes at the oceanic surface. In order to prevent climatic drift the two components are flux-corrected (Sausen et al., 1988), with these corrections varying monthly, but being invariant from year-to-year. Hence they do not influence the inter-annual variability for the simulated climate. The model includes diurnal and seasonal variability as defined by the solar cycle. Inter-annual variability results solely from the nonlinear mechanisms internal to the model. Complex radiative and convective schemes are incorporated in the model, along with the other physical processes designed to represent sub-grid scale phenomena. Thus cloud amount is computed and a gravity wave scheme is incorporated in order to represent dissipation of momentum. The biospheric scheme includes a number of soil and plant types, whose properties vary on a monthly timescale. A rather simple two-layer soil moisture formulation is used.

The sea-ice scheme allows for growth and decay of sea-ice from thermal processes, as well as compaction and thinning of the ice from dynamical processes. The sea-ice can also be transported by oceanic currents or wind forcing.

The oceanic component reproduces the large-scale observed circulations, as well as the deep oceanic features. The ocean plays a critical role in determining the sea surface temperatures (SST) and their variability. The SST in turn are instrumental in defining much of the resultant atmospheric climatology. For a more detailed description of the model formulation and basic climatology see Gordon and O'Farrell (1997).

The major deficiency of the model, common to other models of this generation, is its inability to reproduce the observed range of SST anomalies associated with El Niño/Southern Oscillation (ENSO) events. The model anomalies are slightly over half the observed values. However, the Southern Oscillation is extremely well simulated (Hunt and Elliott, 2003), as are most of the climatic perturbations associated with ENSO events. The model has performed well in international comparisons (AchutaRao and Sperber, 2000; Covey et al., 2000).

The present simulation was initiated from a previous 1,000-year simulation of the model, hence all climatic variables were fully developed. It is emphasized that no external perturbations such as solar fluctuations, volcanic eruptions or changes in greenhouse gas concentrations were permitted during the duration of the 10,000-year long simulation. Thus a simulation of 'present' climate only was obtained. The model output then provides an indication of the magnitude and frequency of climatic fluctuations, and, especially climatic extremes, which are generated solely by processes internal to the climatic system.

3. Simulated Yucatan Climatology

The observed rainfall total in the Yucatan region is about 160 cm/year, with 70–80% of the rainfall occurring between May and October (Aleman and Garcia, 1974). This region is also prone to summer droughts.

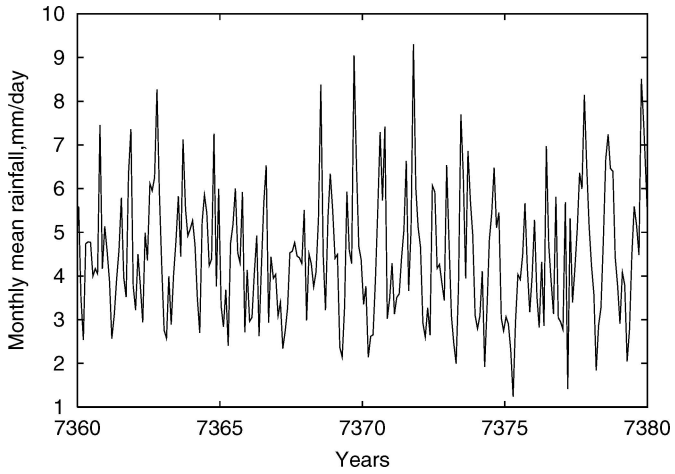

Figure 1. Time series of a sample of monthly rainfall from the 10,000-year simulation for a small Central American region (12°N–22°N, 87°W–94°W).

The model simulated these basic features as illustrated in Figures 1 and 2. Figure 1 shows the seasonal cycle of rainfall averaged over a small region of Central America (12°N–22°N, 87°W–94°W) for a 20-year period that includes the driest year, 7375, for the Yucatan in the 10,000-year simulation. The simulation reproduces noticeable inter-annual variability and some seasonal variability as regards the timing of peak rainfall. The endemic nature of drought in this region can be seen from Figure 1, where in addition to the massive drought in year 7375, there was a further less intense drought in year 7367. The model simulated droughts support the contentions of Dahlin (1983) and Hodell et al. (1995) amongst others, that drought was a major constraint throughout the whole lifespan of Maya civilization.

The spatial pattern of rainfall in the Yucatan region is shown in Figure 2 for January and August conditions for a year of average rainfall, 7350, and the extremely dry year, 7375. Given the minimal rainfall in January, the rainfall differences between these two years are not particularly important. However, in August there is a very marked difference in rainfall amount, highlighting the drought in year 7375.

In order to explore the simulated rainfall characteristics of the Yucatan region a time series of annual mean rainfall anomalies was extracted from the model for just the Yucatan Peninsula, 18°N–22°N, 87°W–92°W. These anomalies are defined as differences from the 10,000-year annual mean. This time series enabled inter-annual variability of rainfall to be scrutinized and extremes to be identified. A small sample of the 10,000-year time series is shown in Figure 3a, which contains the most extreme negative rainfall anomaly of the series centered on year 7375. This time series reveals that multi-year negative rainfall anomalies (droughts) occurred, with an especially notable episode associated with the years around 7375. Single year anomalies can also be identified. The predominance of inter-annual variability is apparent, as documented in other studies with this model (Hunt, 2001).

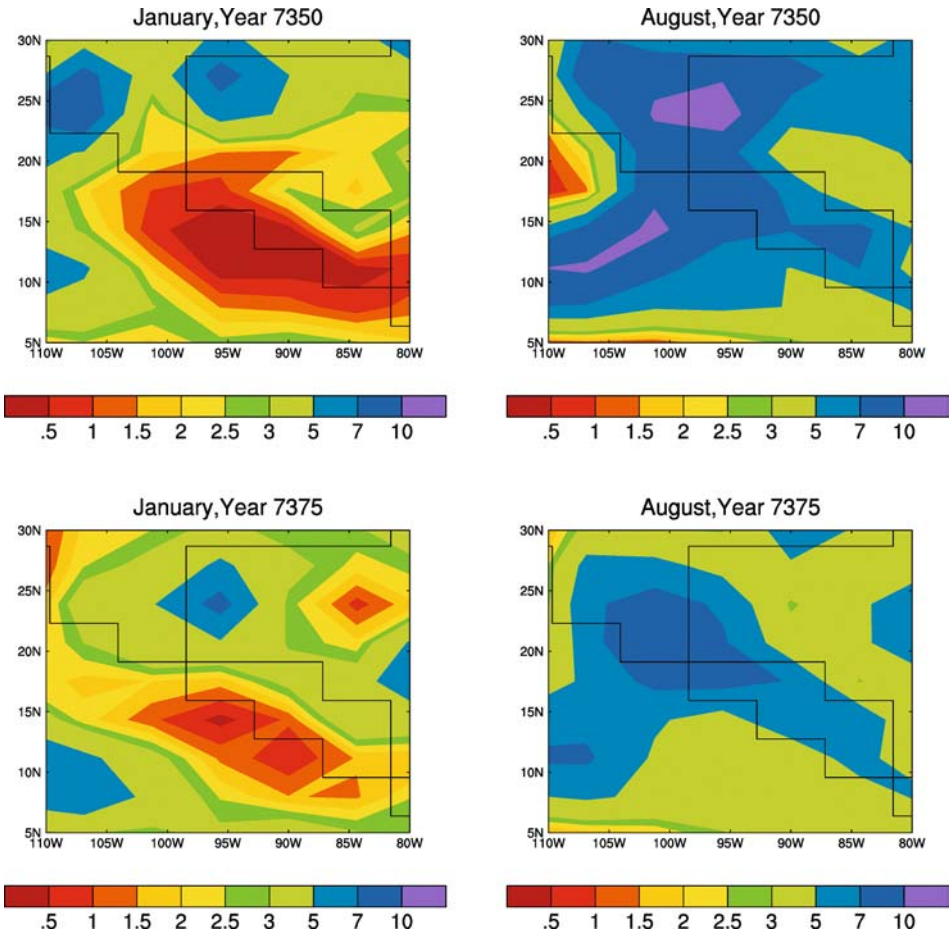

Figure 2. Monthly mean rainfall distributions for the Central American region for a year of average rainfall, year 7350, top panels, and the driest year, year 7375, bottom panels. January and August results are given in the left and right panels, respectively. The colour bar is in mm/day.

Figure 3b presents monthly rainfall anomalies for the Yucatan region. This reveals that the drought in year 7375 extended over the whole year, thus emphasizing why this particular drought was so severe.

A measure of the frequency of severe droughts in the Yucatan region is illustrated in Figure 3c, where normalized rainfall anomalies (rainfall divided by the 10,000-year standard deviation) for magnitudes less than –3 are compared. Twelve events were recorded in the 10,000-year period, but with a very uneven occurrence rate. Thus there was a greater than 2,000-year period with no extreme events, while around 7,000 years three events occurred in close proximity. Haug et al. (2003) report three intense droughts for the Yucatan, at 810, 860 and 910 AD, around the time of the collapse of the Maya civilization, a feature which the model fortuitously

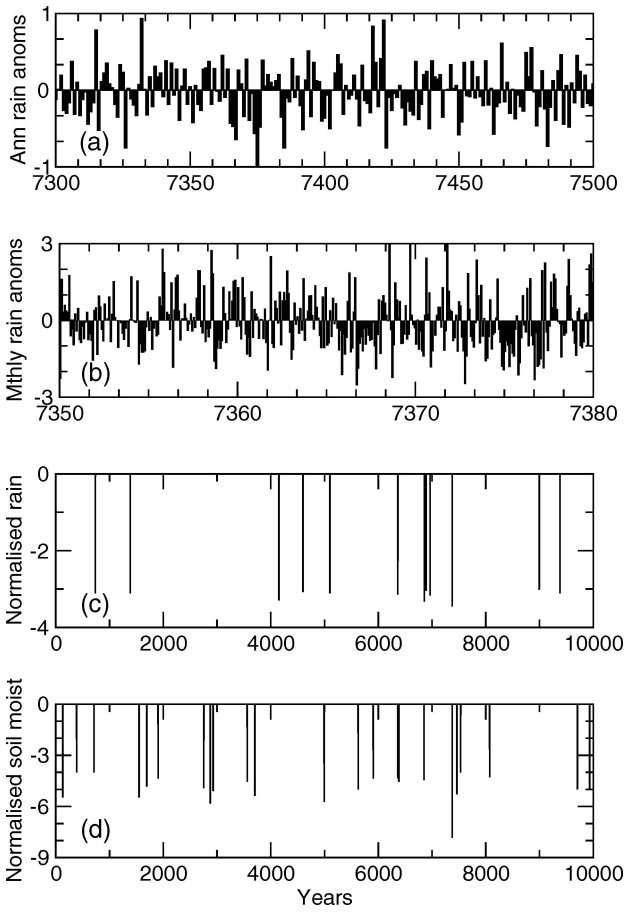

Figure 3. Panel (a). Sample of annual mean rainfall anomalies (all anomalies are differences from the 10,000-year mean) for the Yucatan region (18°N–22°N, 87°W–92°W) highlighting the extreme event at year 7375. (b) A sample of rainfall anomalies at monthly intervals around year 7375. Rainfall anomalies in (a) and (b) are in mm^{-1} day. (c) Normalized annual mean rainfall values (rainfall anomalies divided by the standard deviation of the 10,000-year annual rainfall amounts). Only values less than −3 standard deviations are shown. (d) Normalized annual mean soil moisture values. Only values less than −4 standard deviations are shown.

appears to have simulated. Many less intense droughts occurred at other times in the simulation, as can be judged by Figure 3a.

Finally, Figure 3d compares normalized anomalies of soil moisture content over the 10,000-year simulation for magnitudes below −4. While only a simple two-layer soil moisture scheme is used in the model, it should still be indicative of groundwater variations. Frequent groundwater deficiencies seem to be the characteristic of this region, with an especially severe case occurring in year 7375. It has been suggested (Haug et al., 2003) that access to groundwater was an essential aspect of the survival of the Maya population. Not all the years of severe drought identified in Figure 3c

were associated with the extreme soil moisture deficiencies listed in Figure 3d, as antecedent rainfall was also important in determining whether such deficiencies were attained.

The global distribution of rainfall anomalies for the extreme drought years identified in Figure 3c are plotted in Figure 4. In each of these years a marked negative rainfall anomaly is located over Central America, as would be expected. *In most years the remarkable feature is the very restricted spatial extent of these rainfall anomalies*. The localized nature of the anomalies would suggest that they are in turn generated by *local* climatic perturbations rather than as part of a larger climatic feature such as ENSO events. In fact, examination of the corresponding global surface

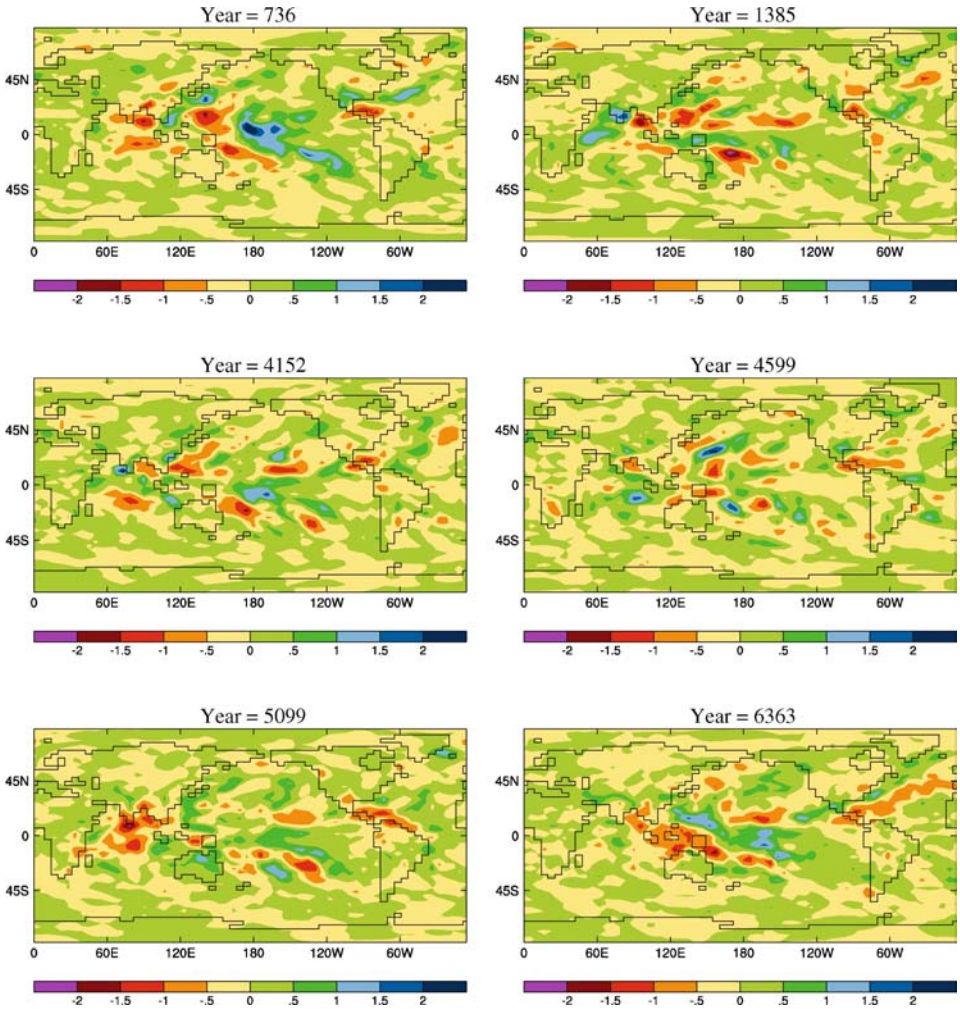

Figure 4. Annual mean rainfall anomalies for extreme drought years in the the Yucatan region identified in Figure 3. The colour bar is in mm^{-1} day. (*Continued on next page*)

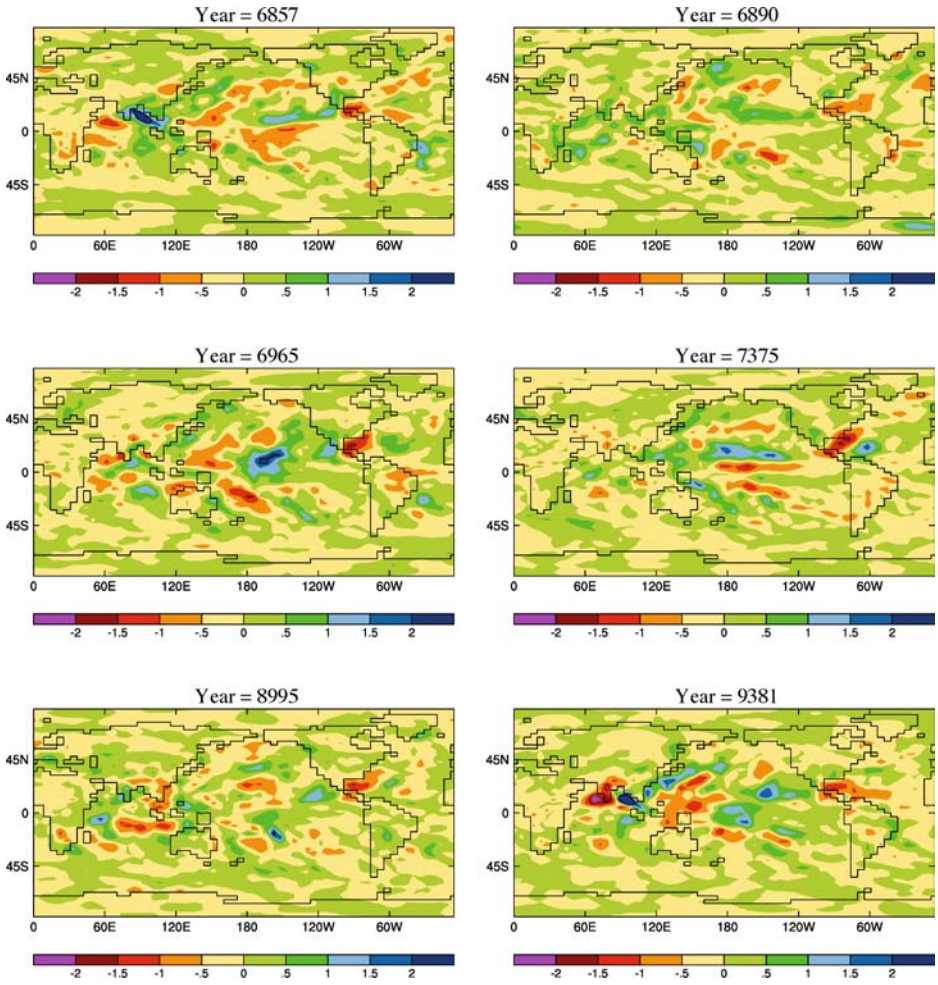

Figure 4. (*Continued*).

temperature anomalies for these years (not shown) revealed a mixture of La Niña and El Niño events occurred. To some extent this can be deduced by the rainfall anomaly patterns over the low latitude Pacific Ocean in Figure 4. Furthermore, there does not seem to be any systematic relationship between the Central American rainfall anomalies and any other region of the globe.

Hodell et al. (2001) noted that drought in the Yucatan in the ninth century was concurrent with drought in the Sahel and low latitudes. This simultaneity with the Sahel has been discussed in some detail by Street-Perrott et al. (2000). In some years as shown in Figure 4, below average rainfall occurred in the Sahel and Middle East, but the relationship is not compelling.

Overall, the outcomes in Figures 3 and 4 certainly support the supposition of Hodell et al. (1995) that major drought could have been instrumental in causing

the termination of the Maya civilization. These figures confirm that major rainfall deficiencies are a systematic, but irregular, characteristic of the Yucatan region.

Given the dominant influence ENSO events exert in observed climatic fluctuations, it was deemed desirable to quantify the role of such events in Yucatan droughts, despite the negative view expressed above.

For example, Ropelewski and Halpert (1987), in an observational study found only a weak ENSO influence on rainfall variability in Central America and the Caribbean. In contrast, Diaz et al. (2001) reported a correlation of about −0.6 for summer conditions, but the reverse sign for late winter/spring, between rainfall for this extended region and an ENSO index. They used rather highly smoothed and processed data to obtain this result. Their correlations over the Yucatan region, see their Plate 2, appear to be much smaller.

Over all 10,000 years of the simulation a correlation of −0.16 was obtained between smoothed (10-point running mean) values of *annual* mean NINO3.4 sea surface temperature and rainfall anomalies for a small region covering the Yucatan and nearby areas (12°–22°N, 87°–94°W). The correlation magnitude was sensitive to the size of region considered. Examination of monthly Yucatan rainfall anomalies revealed considerable month-to-month variability in some years, thus highlighting the problem of obtaining consistent correlations.

The possibility of an ENSO relationship with Yucatan rainfall was further explored by generating a one-point correlation map, whereby rainfall for a single model grid box in the Yucatan was correlated with surface temperatures over the globe, see Figure 5.

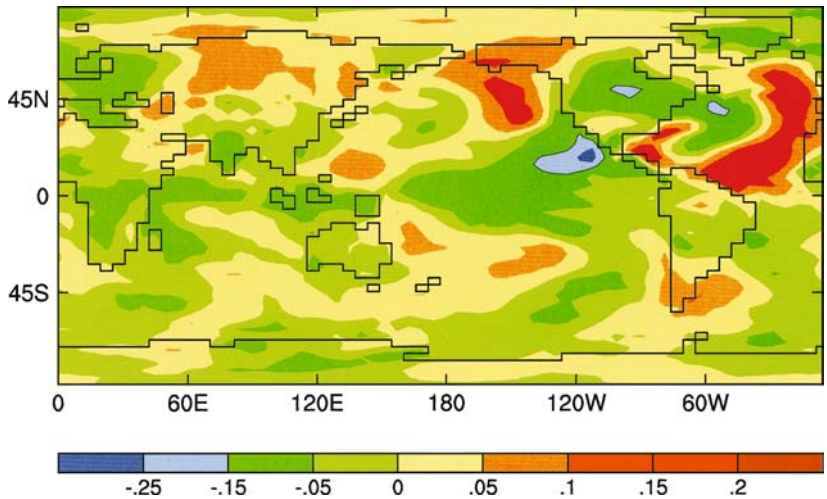

Figure 5. One-point correlation map for rainfall for a single gridbox in the Yucatan region and global surface temperature. Annual mean values for years 7001–8000 were used. The colour bar indicates the magnitude of the correlation coefficient.

The maximum correlations, $\approx |0.25|$, occurred in the Pacific and Atlantic Oceans adjacent to Mexico. Correlations with the low latitude Pacific Ocean and western North Atlantic Oceans are only about -0.1, suggesting little mechanistic connection with Yucatan rain. On the other hand, the magnitude of the maximum correlations, and their spatial extent, imply a very local relationship with Yucatan rainfall. The regions with maximum correlation show that Yucatan rainfall deficits are associated with positive surface temperature anomalies in the Pacific Ocean adjacent to Mexico, and negative anomalies in the corresponding Atlantic Ocean region. The maximum magnitude of these temperature anomalies was 1K. Years with positive rainfall anomalies had reverse patterns of temperature anomalies.

Despite the small correlations over the low-latitude Pacific Ocean in Figure 5, a possibility still exists that the Pacific North America (PNA) oscillation might influence the occurrence of extreme rainfall conditions in the Yucatan. The Mexican region comes under the extremity of the PNA oscillation (Horel and Wallace, 1981). The excitation of this oscillation appears to be associated with a number of possible causes. ENSO events are one possibility (Horel and Wallace, 1981; Hunt and Elliott, 2002), while sea surface temperature perturbations in the North Pacific Ocean and stochastic inputs from the atmosphere are additional possibilities (Lau, 1997; Rodinov and Assel, 2001).

Since the observed and simulated rainfall in the Yucatan peaks in summer, the impact of the PNA oscillation on the Yucatan region was investigated for the mean of July, August and September. Deviations of the 200-mb geo-potential height (an indicator of PNA activity) from the 10,000-year mean were calculated for these months for the 12 extreme events identified in Figure 3c. Typically, this time of year is one of weak response for the PNA Oscillation (Horel and Wallace, 1981), and a range of PNA patterns were obtained (not shown). Many of these patterns had little resemblance to the traditional PNA pattern (Horel and Wallace, 1981), which is optimally obtained for December, January and February, and which the model can simulate extremely well (Hunt and Elliott, 2002). This suggests that PNA/ENSO influences are not dominant as regards perturbations to Yucatan rainfall. This conclusion was reinforced by recomputing the correlations shown in Figure 5 for July, August and September conditions, when similar low correlations were obtained.

Although the spatial extent and magnitude of the surface temperature anomalies, implied in Figure 5, adjacent to Mexico are small, the possibility exists that they could be the cause of the Yucatan rainfall perturbations. However, examination of associated surface wind anomalies suggests otherwise. This is most easily exemplified by consideration of the meridional wind distribution. Figure 6a illustrates the annual mean surface meridional wind distribution for year 7375 (this pattern is essentially invariant with time for the contour intervals used in the figure (see Hunt, 2004)). The important features of this figure as regards the present study are the large, topographically-constrained wind maxima off the west and east coasts of the Americas. In Figures 6b and 6c are the meridional wind anomalies for year 7375

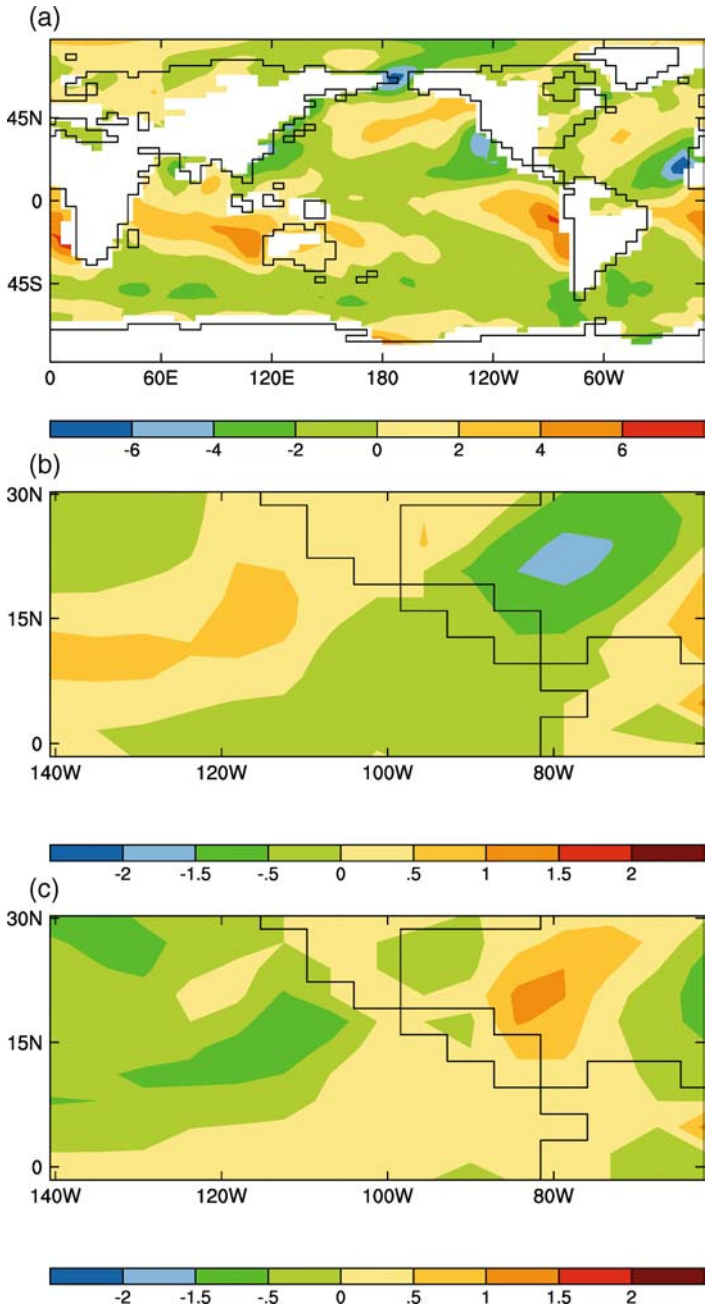

Figure 6. Panel (a) The annual mean meridional wind distribution for the lowest model level (≅300 m) for year 7375 of the simulation. (b) The meridional wind anomalies, as departures from the 10,000-year mean for year 7375, a dry year. (c) Corresponding anomalies for year 3450, a wet year. The colour bar is in m s^{-1}.

(drought year) and year 3450 (a pluvial year), where the spatial pattern displayed has been constrained to the region of interest. Note the reversal of the anomaly patterns between dry and wet years. Superimposing the anomaly distributions of Figure 6b upon the climatological patterns in Figure 6a, it can be seen that the response is to weaken the meridional winds in the Pacific and strengthen them in the Atlantic. The resulting impacts on the oceanic circulations adjacent to Mexico would be to reduce oceanic upwelling of cold water on the west coast, thereby producing a positive sea surface temperature anomaly, and to increase divergence and oceanic mixing on the east coast leading to a negative sea surface temperature anomaly. The opposite responses would be obtained for the pluvial year in Figure 6c. Since these anomalous wind changes would also induce rainfall anomalies over the Yucatan (see below), it appears that both the rainfall and sea surface temperature changes are responding to the same forcing mechanism (meridional wind fluctuations), rather than the former responding to the latter. This would help to explain the low correlations in Figure 5.

Consider now the rainfall anomalies. The Yucatan region comes under the influence of the extension of the Bermuda High (Aleman and Garcia, 1974). The correlation between the rainfall and surface pressure for the Yucatan, using monthly anomalies for all 10,000 years of the simulation, was –0.371. This implies the usual physical relationship where rainfall deficits are associated with high surface pressure and vice versa for rainfall surpluses. In the Yucatan region, the climatological north wind adjacent to the Atlantic coast is enhanced (Figure 6b); in the dry year, consistent with increased outflow associated with the higher surface pressure. This higher surface pressure implies adiabatic descent of the air in this region and thus suppression of rainfall. The reverse situation is indicated for the wet year when the meridional wind anomalies imply reduced outflow, and conditions more conducive to enhanced rainfall. Thus a physically consistent pattern of rainfall, sea surface temperature and meridional wind anomalies is obtained.

Why then do such extreme rainfall deficits (Figure 3) occur over the Yucatan region from time to time? The answer appears to be that these are responses to stochastically induced perturbations in the topographically constrained meridional wind distributions in the American region. This is certainly consistent with the random nature of the extreme rainfall deficiencies shown in Figure 3a. The reason why the Yucatan is so sensitive to stochastic perturbations is that it lies at the interface of these wind distributions.

Assuming drought was a major contributory factor to the Maya downfall, the question arises as to whether there are alternative progenitors to Yucatan drought in addition to the stochastic mechanism proposed here. As discussed above, ENSO influences do not seem to have a consistent or dominant influence on Yucatan rainfall. There appears to be no record in lake cores, for example, (Curtis et al., 1998; Hodel, 1995), that volcanoes perturbed the Yucatan climate. Hodell et al. (2001) have suggested that there is a solar influence on drought in the Yucatan region, but

like most proposals involving the sun it is difficult to identify or formulate plausible mechanistic links.

The stochastic mechanism identified in this paper has a great attraction of inherent simplicity, freedom from contrived climatic linkages and being an integral part of the natural variability of the climatic system.

While population pressures may have contributed to the collapse of the Maya civilization (Haug et al., 2003), it also appears that they were unfortunately associated with an unusual climatic period where several drought episodes occurred within a limited timeframe. Importantly, severe droughts such as discussed here remain an ongoing feature of Yucatan climatology.

4. Concluding Remarks

The proposition of Hodell et al. (1995), based on proxy data, that the collapse of the Maya civilization was caused by drought would appear to be plausible, although it is suggested here that drought-related disease may have accentuated the problem. The present climatic simulation certainly supports this proposition, and highlights the sporadic nature of droughts, presumably severe enough to engender such a collapse. An interesting outcome of the simulation was the geographically restricted nature of these severe droughts. The analysis of the climatic mechanisms associated with these droughts identified internally consistent perturbations in rainfall, sea surface temperature and surface wind anomalies. Certainly, the apparent random nature of the severe droughts is consistent with the hypothesis advanced here that they are caused by stochastically induced fluctuations of the topographically constrained meridional wind systems.

The present simulation, of course, does not *prove* that stochastically forced droughts caused the demise of the Mayans, but it certainly supports such an outcome, and removes the need to seek more contrived solutions.

This study has provided yet another example of how millennial length climatic simulations can complement observations, and aid in interpretation and explanation of major historical climatic anomalies. There would appear to be considerable scope for collaboration between palaeoclimatologists and modellers in investigating past climatic events, especially those associated with major impacts on civilizations.

References

AchutaRao, K. and Sperber, K. R.: 2000, 'El Niño Southern Oscillation in coupled GCMs', PCMDI Report No. 61, PCDMI, Lawrence Livermore Laboratory, Livermore 95440, USA.

Acuna-Soto, R., Romero, L. C., and Maguire, J. H.: 2002, 'Large epidemics of hemorrhagic fevers in Mexico 1545–1818', *Am. J. Trop. Med. Hyg.* **62**, 733–739.

Aleman, P. A. M. and Garcia, E.: 1974, 'The Climate of Mexico', in Bryson, R. A. and Hare, F. K. (eds.) *World Survey of Climatology*, vol. 11, Elsevier, Amsterdam, pp. 345–404.

Coe, M.: 1999, *Breaking the Maya Code*, Thames and Hudson, New York.

Covey, C., AchutaRao, K., Lambert, S. J., and Taylor, K. E.: 2000, 'Intercomparison of present and future climates simulated by coupled ocean-atmosphere GCMs', PCDMI Report No. 66, PCDMI, Lawrence Livermore Laboratory, Livermore 95440, USA.

Curtis, J. H., Brenner, M., Hodell, D. A., Balser, R. A., Islebe, G. A., and Hooghiemstra, H.: 1998, 'A multi-proxy study of Holocene environmental change in the Maya Lowlands of Peten, Guatemala', *J. Paleolimnol.* **19**, 139–159.

Dahlin, B. H.: 1983, 'Climate and prehistory on the Yucatan peninsula', *Clim. Change* **5**, 245–263.

deMonocal, P. B.: 2001, 'Cultural responses to climate change during the Late Holocene', *Science* **292**, 667–673.

Diaz, H. F., Hoerling, M. P., and Eischeid, J. K.: 2001, 'ENSO variability, teleconnections and climate change', *Int. J. Climatol.* **21**, 1845–1862.

Gordon, H. B. and O'Farrell, S. P.: 1977, 'Transient climate change in the CSIRO coupled model with dynamical sea ice', *Mon. Weather Rev.* **125**, 875–907.

Haug,. G. H., Gunther, D., Peterson, C., Sigman, D. M., Hugen, K. A., and Aeschlimann, B.: 2003, 'Climate and the collapse of Maya civilisation', *Science* **299**, 1731–1735.

Hodell, D. A., Curtis, J. H., and Brenner, M.: 1995, 'Possible role of climate in the collapse of Classic Maya civilization', *Nature* **375**, 391–394.

Hodell, D. A., Brenner, M., Curtis, J. H., and Guilderson, T.: 2001, 'Solar forcing of drought frequency in the Maya Lowlands', *Science* **292**, 1367–1370.

Horel, J. D. and Wallace, J. M.: 1981, 'Planetary-scale atmospheric phenomena associated with the Southern Oscillation', *Mon. Weather Rev.* **109**, 813–829.

Hunt, B. G.: 1998, 'National climatic variability as an explanation for historical climatic fluctuations', *Clim. Change* **38**, 133–157.

Hunt, B. G.: 2000, 'Natural climatic variability and Sahelian rainfall trends', *Global Plan. Change* **24**, 107–131.

Hunt, B. G.: 2001, 'A description of persistent climatic anomalies in a 1000-year climatic model simulation', *Clim. Dyn.* **17**, 717–733.

Hunt, B. G. and Elliott, T. I.: 2002, 'Mexican megadrought', *Clim. Dyn.* **20**, 1–12.

Hunt, B. G. and Elliott, T. I.: 2003, 'Secular variability of ENSO events in a 1000-year climatic simulation', *Clim. Dyn.* **20**, 689–703.

Hunt, B. G.: 2004, 'The stationarity of global mean climate', *Int. J. Climatol.* **24**, 795–806.

Lau, N.-C.: 1997, 'Interactions between global SST anomalies and the midlatitude atmospheric circulation', *Bull. Am. Meteorol. Soc.* **78**, 21–33.

Morino Aleman, P. A. and Garcia, E.: 1974, 'The Climate of Mexico', in Bryson, R. A. and Hare, F. K. (eds.), *Climates of North America*, volume 11 of World Survey of Climatology, Elsevier Scientific Publishers, Amsterdam, pp. 345–404.

Rodinov, S. and Assel, R.: 2001, 'A new look at the Pacific/North American Index', *Geophys. Res. Lett.* **28**, 1519–1522.

Ropelewski, C. F. and Halpert, M. S.: 1987, 'Global and regional scale precipitation patterns associated with El Niño/Southern Oscillation', *Mon. Weather Rev.* **115**, 1606–1626.

Sausen, R., Barthel, K., and Hasselmann, K.: 1988, 'Coupled ocean-atmosphere models with flux correction', *Clim. Dyn.* **2**, 145–163.

Street-Perrott, F. A., Holmes, J. A., Waller, M. P., Allen, M. J., Barber, N. G. H., Fothergill, P. A., Harkness, D. D., Ivanovich, M., Kroon, D., and Perrolt, R. A.: 2000, 'Drought and dust deposition in the West African Sahel: A 5500-years record from Kajemarum Oasis, northeastern Nigeria', *The Holocene* **10**, 293–302.

(Received 3 June 2003; in revised form 17 June 2004)